Quantum phase transition between orbital-selective Mott states in Hund's metals

Julián Rincón,[1,2] Adriana Moreo,[2,3] Gonzalo Alvarez,[1,4] and Elbio Dagotto[2,3]

[1]*Center for Nanophase Materials Sciences, Oak Ridge National Laboratory, Oak Ridge, Tennessee 37831, USA*
[2]*Materials Science and Technology Division, Oak Ridge National Laboratory, Oak Ridge, Tennessee 37831, USA*
[3]*Department of Physics and Astronomy, The University of Tennessee, Knoxville, Tennessee 37996, USA*
[4]*Computer Science and Mathematics Division, Oak Ridge National Laboratory, Oak Ridge, Tennessee 37831, USA*

We report a quantum phase transition between orbital-selective Mott states, with different localized orbitals, in a Hund's metals model. Using the density matrix renormalization group, the phase diagram is constructed varying the electronic density and Hubbard U, at robust Hund's coupling. We demonstrate that this transition is preempted by charge fluctuations and the emergence of free spinless fermions, as opposed to the magnetically driven Mott transition. The Luttinger correlation exponent is shown to have a universal value in the strong-coupling phase, whereas it is interaction dependent at intermediate couplings. At weak coupling we find a second transition from a normal metal to the intermediate-coupling phase.

Introduction. Hund's metals (HM) are strongly interacting quantum states with bad metallic properties, where electronic correlations are dominated by the Hund's coupling J and not by the Hubbard repulsion U. HM are stable in intermediate coupling regimes, within two energy scales [1–3]. A weak-coupling scale signals a transition from a bad to a coherent metal, i.e., a Fermi liquid (FL). The second (strong-coupling) characteristic energy separates the incoherent metal from an ordered phase [1–6]. HM display a variety of phenomena: mass enhancement [1], orbital selectivity [7,8], suppression of orbital fluctuations [8], emergence of local moments [4], and non-Fermi-liquid (NFL) physics [1–3].

Early work unveiled the freezing of local moments and power-law behavior in the electronic self-energy, using dynamical mean-field theory (DMFT) applied to a three-orbital Hubbard model [4]. A related orbital-dependent power law in the self-energy and optical conductivity was reported in DFT + DMFT studies [2]. These results were discussed in the context of iron-chalcogenide and ruthenate superconductors suggesting that these materials are governed by Hund's physics [3,9–11]. Using effective low-energy Kondo Hamiltonians with orbital degrees of freedom, the FL-NFL (coherent-incoherent) transition observed in those compounds was explained [2,5,6,12].

The orbital-selective Mott phase (OSMP) is an example where Hund physics plays a crucial role. The OSMP is a bad metal where Mott insulator (MI) and normal metal coexist, leading to a NFL [3,9]. This exotic behavior is due to the orbital-decoupling effect induced by J, suppressing orbital fluctuations. In the low-energy sector, the OSMP is described by a double-exchange model: a ferromagnetic Kondo lattice with band interactions [9,12,13], which displays NFL. The conditions for a stable OSMP have been thoroughly discussed using several techniques [3,8,14–20].

Studies of the magnetic order in the OSMP have shown a tendency to ordered phases such as paramagnetism (PM), ferromagnetism (FM), antiferromagnetism (AFM) [21], and block states (FM clusters coupled AFM). One of the properties of the OSMP state recently explored are its magnetic and charge orders: block states and FM were found in the spin sector and short-range order in the charge sector [13].

The OSMP has an associated orbital-selective Mott transition to a MI. This transition was first proposed to explain the coexistence of metallic and magnetic behavior in ruthenates [7]. The origin of the orbital-selective Mott transition is mainly related to a strong J and its band-decoupling effect [8]; however, crystal-field splitting [22] and unequal bandwidths are other factors that may lead to orbital differentiation and an orbital-selective Mott transition, in systems poorly hybridized. These findings were considered in the context of iron-based superconductors [3,8,9,13,22–30].

In this Rapid Communication we explore the influence of carrier doping and U on an OSMP, employing a three-orbital Hubbard model and the density matrix renormalization group (DMRG) [31–33]. Our main result is the discovery of a formerly unknown quantum phase transition (QPT) between OSMPs (OSMP QPT) with different localized orbitals. We argue that this QPT is preceded by charge fluctuations and not magnetic fluctuations, and by the appearance of spinless fermions establishing a qualitative difference with the Mott transition. Calculations of the Luttinger liquid correlation exponent show a universal behavior in the strong-U OSMP. We also find a small-U QPT between a normal metal and an OSMP. This physics could be realized in heavy-fermion and iron-based compounds with tendencies to Hund's metallicity.

Model and method. The model used in our study is a one-dimensional three-orbital Hubbard Hamiltonian. The details of the model were given elsewhere [34], but here we briefly describe its main features. The Hamiltonian is divided as $H = H_{kin} + H_{int}$. The kinetic energy, H_{kin}, includes hopping among orbitals γ and an orbital-dependent crystal-field splitting term. The interacting part, H_{int}, is composed of the intraorbital (U) and interorbital (U') Coulomb repulsions, the FM Hund's coupling (J), and the pair-hopping term [35].

The parameters in H_{kin} were chosen to mimic the band structure of the iron-based compounds [36]. We fix the ratio $J/U = 1/4$, a prototypical value used in the study of multiorbital systems, and explore the phase diagram by changing the electronic filling in the range $3 \leqslant n \leqslant 5$ and varying U. The total bandwidth is $W = 2.45$ eV. Our conclusions are drawn from DMRG calculations of the orbital occupation number n_γ, the magnetic moment $\langle \mathbf{S}^2 \rangle$, the charge $N(q)$ and spin $S(q)$
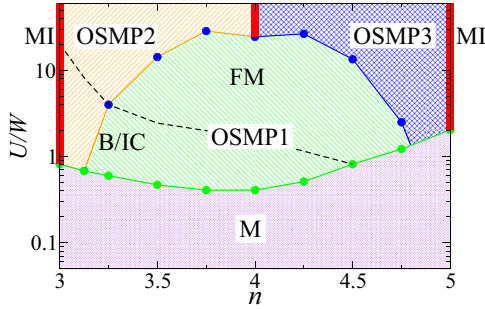
FIG. 1. (Color online) DMRG phase diagram of the three-orbital model varying U/W and n, at $J/U = 1/4$ for a 72-orbital lattice. The phases are labeled as metal (M), Mott insulator (MI), and orbital-selective Mott phase (OSMP). In the OSMPs, block/incommensurate (B/IC) magnetism and ferromagnetism (FM) are separated by a dashed line. The quantum phase transitions are separated by the full lines.

structure factors, and the orbital-dependent Luttinger liquid parameter K_γ. The truncation error was $< 10^{-4}$; finite-size effects in the phase diagram are small [34].

Results. We calculated the phase diagram of our multiorbital model varying U and n [37]. The phase diagram is shown in Fig. 1. At integer n and $U/W \gtrsim 1$, a MI with AFM is found (thick bars). For all values of n and $U/W \lesssim 1$, a PM-M state is observed. Now one of the main results of our work: At intermediate and strong U, we detect phases with similar characteristics to those of the OSMP; specifically, three types of OSMPs are uncovered. (i) At intermediate U we observe an OSMP with two metallic (itinerant) orbitals and *one localized* orbital (OSMP1). (ii) At strong coupling and dependent on n, we unveil two new types of OSMPs. For $3 < n < 4$ the OSMP is characterized by the coexistence of one metallic orbital and *two localized* orbitals (OSMP2). By contrast, for $4 < n < 5$ we observe an OSMP with one itinerant, *one filled, and one localized* orbital, which translates to an effective two-orbital OSMP with one metallic and one MI orbital (OSMP3).

The OSMP states display a nontrivial magnetic ordering: Fully saturated FM is found in all of them, and block or incommensurate magnetism is seen in the OSMP1 and OSMP2 phases. Magnetic order was previously overlooked in mean-field studies of the OSMP; however, DMRG allows one to address issues of order. Moreover, though it is not explicitly shown, we have found regions of phase separation, where AFM and FM coexist, near $n = 3$ and 5. The magnetic orders reported in this work agree with those found in previous studies of the two-dimensional double-exchange model, which is the low-energy effective model of the OSMP [38–40], providing a connection with long-range ordered systems.

The emergence of different OSMPs can be deduced by monitoring the orbital occupation, n_γ, vs U/W (shown in Fig. 2 for $n = 3.25$ and 4.5). In the small-U region n_γ exhibits a normal metal. As U/W is increased n_2 locks to one, signaling the appearance of a MI in such orbital at intermediate coupling, while the other orbitals remain itinerant. This is the OSMP1 state shown in Fig. 1. Upon further increase of U two different states develop depending on n. As shown in Fig. 2(a) at $n = 3.25$, n_1 also localizes leaving only one orbital ($\gamma = 0$)
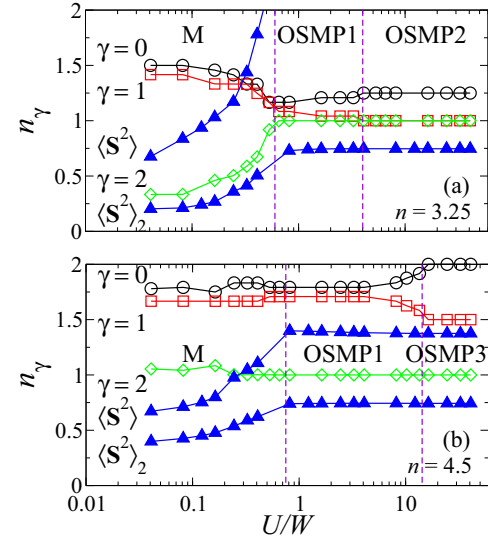

FIG. 2. (Color online) Orbital occupation number n_γ (open symbols), and mean value of the total spin squared, $\langle \mathbf{S}^2 \rangle$ (closed symbols), vs U/W, at $J/U = 1/4$ for (a) $n = 3.25$ and (b) $n = 4.5$. $\langle \mathbf{S}^2 \rangle_2$ is the magnetic moment for $\gamma = 2$. The different phases are marked by vertical dashed lines. Notice the formation of a robust magnetic moment and a fairly U-independent n_γ in the OSMP region.

metallic; this is the OSMP2 state shown in Fig. 1. At $n = 4.5$, plotted in Fig. 2(b), n_1 becomes doubly occupied, making it an inert orbital and inducing an OSMP with one localized and one itinerant orbital: This is the large-U OSMP3 state shown in Fig. 1. One remarkable feature of the OSMP is that n_γ is U independent, but dependent on J, and strongly orbitally differentiated. The existence of the OSMP is further confirmed by the calculation of K_γ (see Fig. 3) [34].

Figure 2 also displays the magnetic moment $\langle \mathbf{S}^2 \rangle$ vs U. In the metallic region we find a small $\langle \mathbf{S}^2 \rangle$ as expected for a PM. In contrast, the OSMPs present a robust moment; this is true regardless of the value of the doping in the region $3 < n < 5$. The presence of a robust moment is a typical feature of the
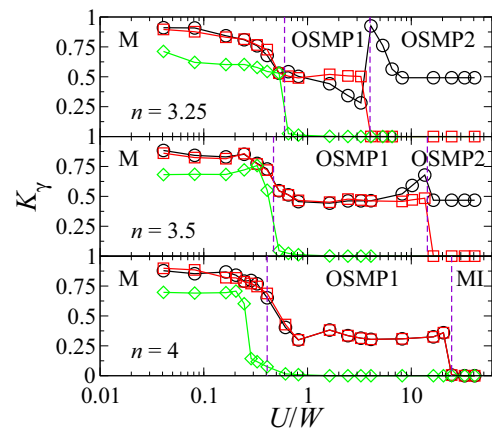

FIG. 3. (Color online) Orbital-dependent Luttinger correlation exponent K_γ, varying U/W, for several fillings n and $J/U = 1/4$. Note the existence of orbital-selective incompressible states ($K_\gamma = 0$). The discontinuities correspond to quantum phase transitions.

OSMP. The value of $\langle \mathbf{S}^2 \rangle$ can be understood by considering the one-body contribution of each orbital. In the OSMP2, the occupations (in terms of holes because the system is above half-filling) are $n_0 = 0.75$, $n_1 = n_2 = 1$ giving an effective $S_{\text{eff}} \approx 1.375$ or $\langle \mathbf{S}^2 \rangle = 3.266$ which is fairly close to the actual value 3.3125. The same argument holds for $n = 4.5$, where $S_{\text{eff}} \approx 1.313$ which is to be compared with 1.375. These results agree nicely with the idea of the orbital-decoupling effect of J.

Assuming that the OSMP metallicity can be described by the universality class of the Luttinger liquid, we have calculated the correlation exponent K_γ which completely characterizes this theory. Figure 3 shows the orbital-dependent K_γ as a function of U/W for several n. To avoid subtleties in the interpretation of K_γ, we have set the orbital hybridization to zero in H_{kin} [34]. In the metallic region, we find that K_γ is strongly orbital dependent (Fig. 2). This tendency is caused by the fact that by changing U/W the filling n_γ effectively changes as well, in a similar way as K depends on n for the single-orbital Hubbard model [41,42]. By further increasing U, a critical line is crossed ($K_2 = 0$) signaling an incompressible state (MI); on the other hand, the metallic orbitals become more correlated: $K_\gamma^{\text{M}} > K_\gamma^{\text{OSMP}}$. With further increasing U, the second OSMP (for $n \neq 4$) or the MI (for $n = 4$) is reached, where $K_1 = K_2 = 0$, $K_1 \to 1/2$ and $K_\gamma = 0$, respectively. The presence of discontinuities in K_γ are the result of different QPTs to different OSMPs.

Note that in the metallic region we found $1/2 < K_\gamma < 1$, resembling results for the standard Hubbard model [41,42]. In contrast, in the strong-coupling OSMP $K_\gamma = 1/2$ or $K_\gamma = 0$, which implies the onset of spinless fermions or an insulator, respectively (see below). One important conclusion can then be drawn from the behavior of K_γ: The strong-U OSMP belongs to the universality class of *free spinless fermions*. Calculating K_γ with the DMRG is a challenging task because we need the long-range behavior of the correlations, which requires accurate calculations for large systems; therefore, the value of K_γ calculated here should be considered as an upper limit to the thermodynamic value.

The origin of the OSMP QPT can be understood by monitoring the charge fluctuations across the transition. The total-charge structure factor $N(q)$, for different n and U (color coded), is shown in Fig. 4. For *noninteger n*, a general tendency is observed: As U increases charge fluctuations are gradually suppressed until U reaches the critical value of the OSMP QPT, and subsequently $N(q)$ takes the form of free spinless fermions. On the contrary, for $n = 4$ where an orbital-selective Mott transition occurs, charge fluctuations are completely suppressed as $U \to \infty$. Unlike the Mott transition where charge fluctuations are almost completely frozen, in the novel OSMP QPT they still play a key role in describing the low-energy properties, where a correlated FM Kondo lattice arises as the effective model of the OSMP1, indicating entanglement between charge and spin [12,13]. It is important to remark that close to the OSMP QPT magnetic fluctuations are frozen, whereas for the orbital-selective Mott transition there is a change from FM to AFM (see Fig. 5).

The origin of the large-U free-spinless-fermion behavior is different from that of the standard Hubbard model. For $U \to \infty$, all the electrons in each orbital, at a given site, will
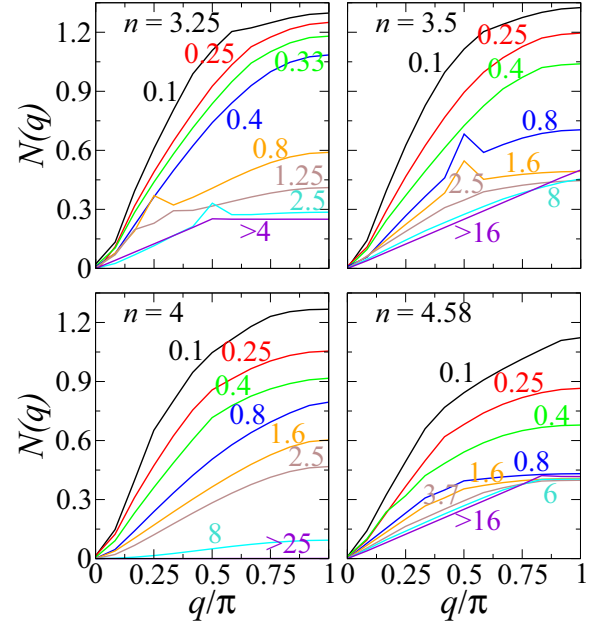

FIG. 4. (Color online) Total-charge structure factor $N(q)$ for several n (panels) at $J/U = 1/4$. Each panel shows $N(q)$ for different U (color coded). Charge fluctuations are suppressed as U/W increases, though not completely and depending on n. The quantum phase transition between orbital-selective Mott states is signaled by the onset of free spinless behavior with an n-dependent effective Fermi momentum.
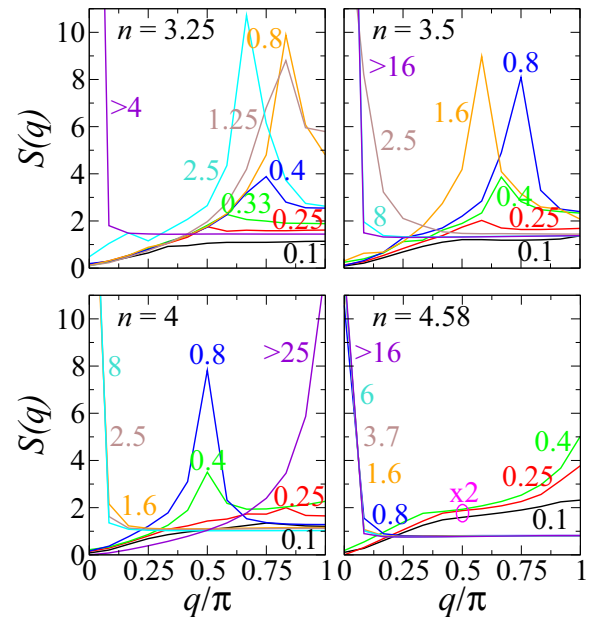

FIG. 5. (Color online) Total-spin structure factor $S(q)$ for the same parameters as in Fig. 4. Data sets are color coded with the corresponding value of U/W. Magnetic orders found are ferromagnetism (FM), block/incommensurate magnetism (B/IC), and for integer n also antiferromagnetism (AFM). The magnitude fluctuations across the phase transition between orbital-selective Mott states remains largely unaffected showing that the transition is driven by charge fluctuations.

form unbreakable local triplets freezing charge fluctuations and effectively hopping as spinless electrons implying spin-charge separation and a drastic change of the screening properties of the low-energy FM Kondo lattice. The OSMP2 is different from the OSMP1 because the itinerant electrons do not effectively have spin and there are *two* orbitals localized. Indeed Anderson and Hasegawa showed that for double-exchange models with $J \to \infty$ the resulting behavior is that of spinless particles [43]. Note that the effective Fermi momentum k_F^{eff} of the spinless fermions will depend on n. The resulting k_F^{eff} can be extracted from the effective filling of the itinerant orbital of the strong-U OSMP. For $n = 3.25$, $\gamma = 0$ is quarter-filled leading to $k_F^{\text{eff}} = \pi/2$; for $n = 3.5$, $\gamma = 0$ is half-filled implying $k_F^{\text{eff}} = \pi$ (see Fig. 2). However, incommensurate k_F^{eff}/π are also possible, and Fig. 4 shows this for $n = 4.58$ which translates to $k_F^{\text{eff}} \approx 0.84\pi$; notice that in this case it is $\gamma = 1$ that is responsible for the spinless behavior, similar to $n = 4.5$ shown in Fig. 2 [34].

Therefore, contrary to the orbital-selective Mott transition where the MI is preempted by AFM fluctuations, the OSMP QPT is preceded by the onset of charge order. Since the original model includes spinful electrons, the resulting spinless behavior corresponds to a nontrivial highly interacting state. To the best of our knowledge, such example of charge-fluctuation-enhanced Mott transition has never been reported.

Along with the OSMP QPT, we detected a small-U stage from normal metal to OSMP. This QPT presents enhancement of charge and magnetic fluctuations (see Figs. 4 and 5). The enhancement manifests as peak changes close to the transition. A similar two-stage evolution from MI to OSMP to normal metal was reported in studies of chalcogenides [2].

The magnetic states found in Fig. 1 are plotted in Fig. 5, for the same parameters as in Fig. 4. For $n = 4$, we found FM, block, and AFM, as formerly reported [13]. For $n \neq 4$, we also found incommensurate magnetism which is characterized by peaks at fractional momenta in $S(q)$. As U increases the general trend consists of moving from a small-U PM to a block/incommensurate at intermediate U, to a large-U FM ($n \neq 4$) or AFM ($n = 4$). For the metal-OSMP QPT there is a change from PM to either block/incommensurate or FM. Thus, this transition is driven by magnetic fluctuations. An entirely different situation is observed in the OSMP QPT, where $S(q)$ does not change across the transition. We notice that for $n \sim 4$, blocks of two- and three-site FM islands are found.

There is a caveat for the existence of the OSMP QPT: The presence of a FM state is necessary. Once FM is established the transition can occur. This can be seen by comparing $n = 3.25$, where the transition happens simultaneously with an incommensurate-FM transition, and $n = 3.5$ or 4.5, where for an already existent FM state the transition occurs regardless of the magnetic fluctuations. Furthermore, the presence of phase separation around $n \gtrsim 3$ prevents its existence. The transition reported here is a generalized form of the orbital-selective Mott transition previously reported [8].

We have confirmed our findings not only for $J/U = 1/4$ but also for other ratios [34]. The specific critical U_c/W required for the OSMP QPT are dependent on J/U. Note that these values are specific to a one-dimensional model with a specific hopping set. Our goal is to establish, via a generic example, that OSMP-OSMP transitions are possible as a matter of principle, while specific realizations in real materials will surely require adjusting hoppings and likely dimensionality.

Conclusions. Using the DMRG, we report a QPT between OSMP states in a Hund's metals model. We have shown that this transition is signaled by furnishing of spinless-fermion behavior meaning that the transition is driven by charge and not magnetic fluctuations. The Luttinger liquid correlation exponent shows a universal value in the strong-U OSMP and a weak interaction-dependent value at intermediate coupling. A small-U transition from normal metal to OMSP is also found. These two transitions are similar to those found in realistic models for heavy-fermion and iron-based compounds.

---

[1] K. Haule and G. Kotliar, New J. Phys. **11**, 025021 (2009).

[2] Z. P. Yin, K. Haule, and G. Kotliar, Nat. Mater. **10**, 932 (2011); Phys. Rev. B **86**, 195141 (2012).

[3] A. Georges, L. de' Medici, and J. Mravlje, Annu. Rev. Condens. Mattter Phys. **4**, 137 (2013).

[4] P. Werner, E. Gull, M. Troyer, and A. J. Millis, Phys. Rev. Lett. **101**, 166405 (2008).

[5] S. Akhanjee and A. M. Tsvelik, Phys. Rev. B **87**, 195137 (2013).

[6] C. Aron and G. Kotliar, arXiv:1401.0331.

[7] V. I. Anisimov, I. A. Nekrasov, D. E. Kondakov, T. M. Rice, and M. Sigrist, Eur. Phys. J. B **25**, 191 (2002).

[8] L. de' Medici, Phys. Rev. B **83**, 205112 (2011).

[9] M. Vojta, J. Low. Temp. Phys. **161**, 203 (2010).

[10] N. Lanatà, H. U. R. Strand, G. Giovannetti, B. Hellsing, L. de' Medici, and M. Capone, Phys. Rev. B **87**, 045122 (2013).

[11] F. Hardy, A. E. Böhmer, D. Aoki, P. Burger, T. Wolf, P. Schweiss, R. Heid, P. Adelmann, Y. X. Yao, G. Kotliar, J. Schmalian, and C. Meingast, Phys. Rev. Lett. **111**, 027002 (2013).

[12] S. Biermann, L. de' Medici, and A. Georges, Phys. Rev. Lett. **95**, 206401 (2005).

[13] J. Rincón, A. Moreo, G. Alvarez, and E. Dagotto, Phys. Rev. Lett. **112**, 106405 (2014).

[14] A. Liebsch, Phys. Rev. B **70**, 165103 (2004).

[15] P. Werner, E. Gull, and A. J. Millis, Phys. Rev. B **79**, 115119 (2009).

[16] H. Ishida and A. Liebsch, Phys. Rev. B **81**, 054513 (2010).

[17] A. Liebsch, Phys. Rev. B **84**, 180505(R) (2011).

[18] L. de' Medici, J. Mravlje, and A. Georges, Phys. Rev. Lett. **107**, 256401 (2011).

[19] E. Bascones, B. Valenzuela, and M. J. Calderón, Phys. Rev. B **86**, 174508 (2012).

[20] M. Greger, M. Kollar, and D. Vollhardt, Phys. Rev. Lett. **110**, 046403 (2013).

[21] C.-K. Chan, P. Werner, and A. J. Millis, Phys. Rev. B **80**, 235114 (2009).

[22] L. de' Medici, S. R. Hassan, M. Capone, and X. Dai, Phys. Rev. Lett. **102**, 126401 (2009).

[23] R. Yu, J.-X. Zhu, and Q. Si, Phys. Rev. Lett. **106**, 186401 (2011).

[24] R. Yu and Q. Si, Phys. Rev. B **86**, 085104 (2012).

[25] M. Yi, D. H. Lu, R. Yu, S. C. Riggs, J.-H. Chu, B. Lv, Z. K. Liu, M. Lu, Y. T. Cui, M. Hashimoto, S.-K. Mo, Z. Hussain, C.-W. Chu, I. R. Fisher, Q. Si, and Z.-X. Shen, Phys. Rev. Lett. **110**, 067003 (2013).

[26] Q. Luo, A. Nicholson, J. Rincón, S. Liang, J. Riera, G. Alvarez, L. Wang, W. Ku, G. D. Samolyuk, A. Moreo, and E. Dagotto, Phys. Rev. B **87**, 024404 (2013).

[27] R. Yu and Q. Si, Phys. Rev. Lett. **110**, 146402 (2013).

[28] L. de' Medici, G. Giovannetti, and M. Capone, Phys. Rev. Lett. **112**, 177001 (2014).

[29] J. M. Caron, J. R. Neilson, D. C. Miller, A. Llobet, and T. M. McQueen, Phys. Rev. B **84**, 180409(R) (2011).

[30] J. M. Caron, J. R. Neilson, D. C. Miller, K. Arpino, A. Llobet, and T. M. McQueen, Phys. Rev. B **85**, 180405(R) (2012).

[31] S. R. White, Phys. Rev. Lett. **69**, 2863 (1992); Phys. Rev. B **48**, 10345 (1993).

[32] U. Schollwöck, Rev. Mod. Phys. **77**, 259 (2005).

[33] K. Hallberg, Adv. Phys. **55**, 477 (2006).

[34] See Supplemental Material at http://link.aps.org/supplemental/10.1103/PhysRevB.90.241105 for details of the definition of model, physical quantities, and additional numerical results.

[35] M. Daghofer, A. Nicholson, A. Moreo, and E. Dagotto, Phys. Rev. B **81**, 014511 (2010).

[36] Our results are, however, quite general as the presence of the OSMP has been shown for different band structures modeling heavy fermions, chalcogenides, and selenides. See Refs. [2, 13, 15, 22, 27].

[37] Notice that the phase boundaries will not qualitatively change if the hybridization is set to zero. This is particularly true for the OSMP, where the relevant energy scales are U and J, and orbital decoupling occurs (see Refs. [8, 22]). The effect of V can also be understood realizing that the low-energy theory of the OSMP is FM Kondo lattice, where such term is absent.

[38] A. J. Millis, P. B. Littlewood, and B. I. Shraiman, Phys. Rev. Lett. **74**, 5144 (1995); A. Chattopadhyay, A. J. Millis, and S. Das Sarma, Phys. Rev. B **64**, 012416 (2001).

[39] J. Riera, K. Hallberg, and E. Dagotto, Phys. Rev. Lett. **79**, 713 (1997); S. Yunoki, J. Hu, A. L. Malvezzi, A. Moreo, N. Furukawa, and E. Dagotto, *ibid.* **80**, 845 (1998).

[40] H. Aliaga, B. Normand, K. Hallberg, M. Avignon, and B. Alascio, Phys. Rev. B **64**, 024422 (2001).

[41] H. J. Schulz, Phys. Rev. Lett. **64**, 2831 (1990).

[42] T. Giamarchi, *Quantum Physics in One Dimension* (Clarendon Press, Oxford, 2004).

[43] P. W. Anderson and H. Hasegawa, Phys. Rev. **100**, 675 (1955).